

PERFORMANCE ANALYSIS AND SIMULATION OF
THE SPS REFERENCE PHASE CONTROL SYSTEM*

W. C. Lindsey and C. M. Chie
LinCom Corporation

ABSTRACT

This short paper provides a summary overview of the SPS reference phase control system as defined in a three phase study effort (see Refs. 1-5). It serves to summarize key results pertinent to the SPS reference phase control system design. These results are a consequence of extensive system engineering tradeoffs provided via mathematical modeling, optimization, analysis and the development/utilization of a computer simulation tool called SOLARSIM.

1.0 INTRODUCTION

The SPS reference phase control system investigated under contract to the Johnson Space Center is reviewed in Section 2. The next section is devoted to the analysis and selection of the pilot signal and power transponder. The SOLARSIM program development and the simulated SPS phase control performance are treated in Section 4.

2.0 THE SPS CONCEPT AND THE REFERENCE PHASE CONTROL SYSTEM

Figure 2.1 illustrates the major elements required in the operation of an SPS system which employs retrodirectivity as a means of automatically pointing the beam to the appropriate spot on the Earth. From Figure 2.1 we see that these include: (1) the transmitting antenna, hereafter called the spacetenna, (2) the receiving antenna, hereafter called the rectenna, and (3) the pilot signal transmitter. The rectenna and pilot signal transmitter are located on the Earth. The purpose of the spacetenna is to direct the high-power beam so that it comes into focus at the rectenna. The pilot signal, transmitted from the center of the rectenna to the spacetenna, provides the signal needed at the SPS to focus and steer the power beam.

As seen from Fig. 2.1 the SPS phase control system is faced with several key problems. They include: (1) path delay variations due to imperfect SPS circular orbits, (2) ionospheric effects, (3) initial beam forming, (4) beam pointing, (5) beam safin, (6) high power amplifier phase noise effects, (7) interference (unintentional and intentional), etc.

2.1 SPS-Transmitting System Concept

From the system engineering viewpoint, the SPS transmitting system which incorporates retrodirectivity is depicted in Fig. 2.2. As seen

*This work was performed at LinCom Corporation for NASA Johnson Space Center Houston, TX, under contract NAS 9-15782.

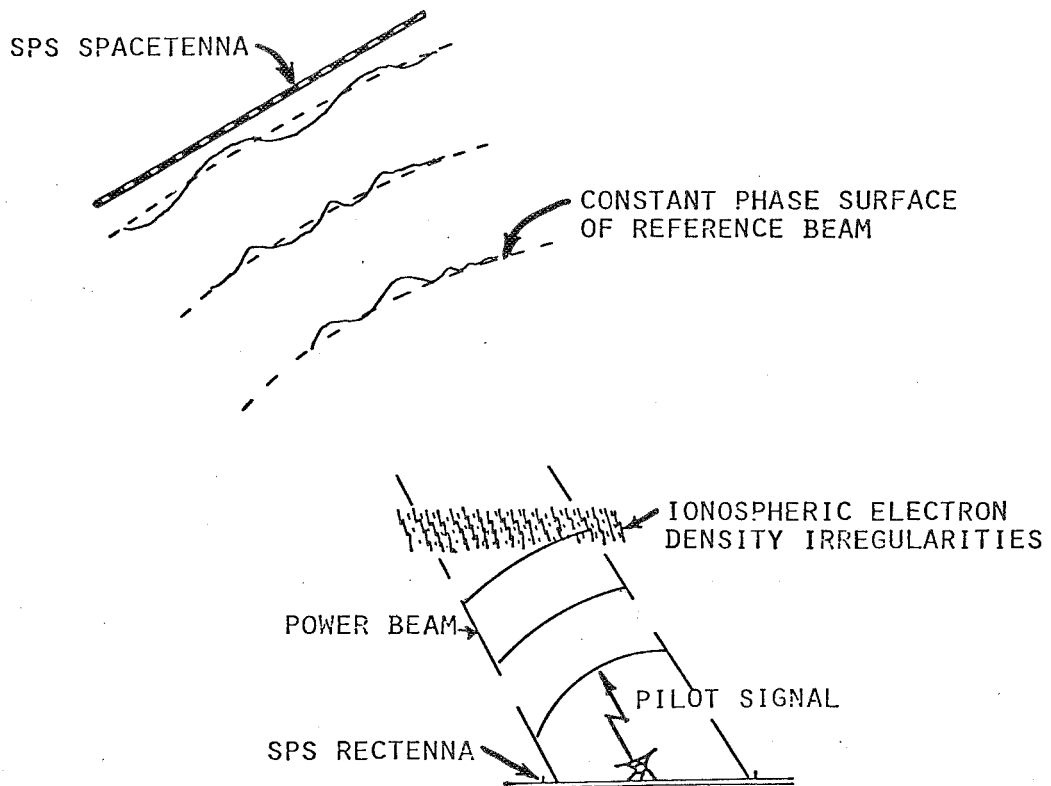


Figure 2.1. Space Based Solar Power Satellite and Earth Based Energy Collection System Concept.

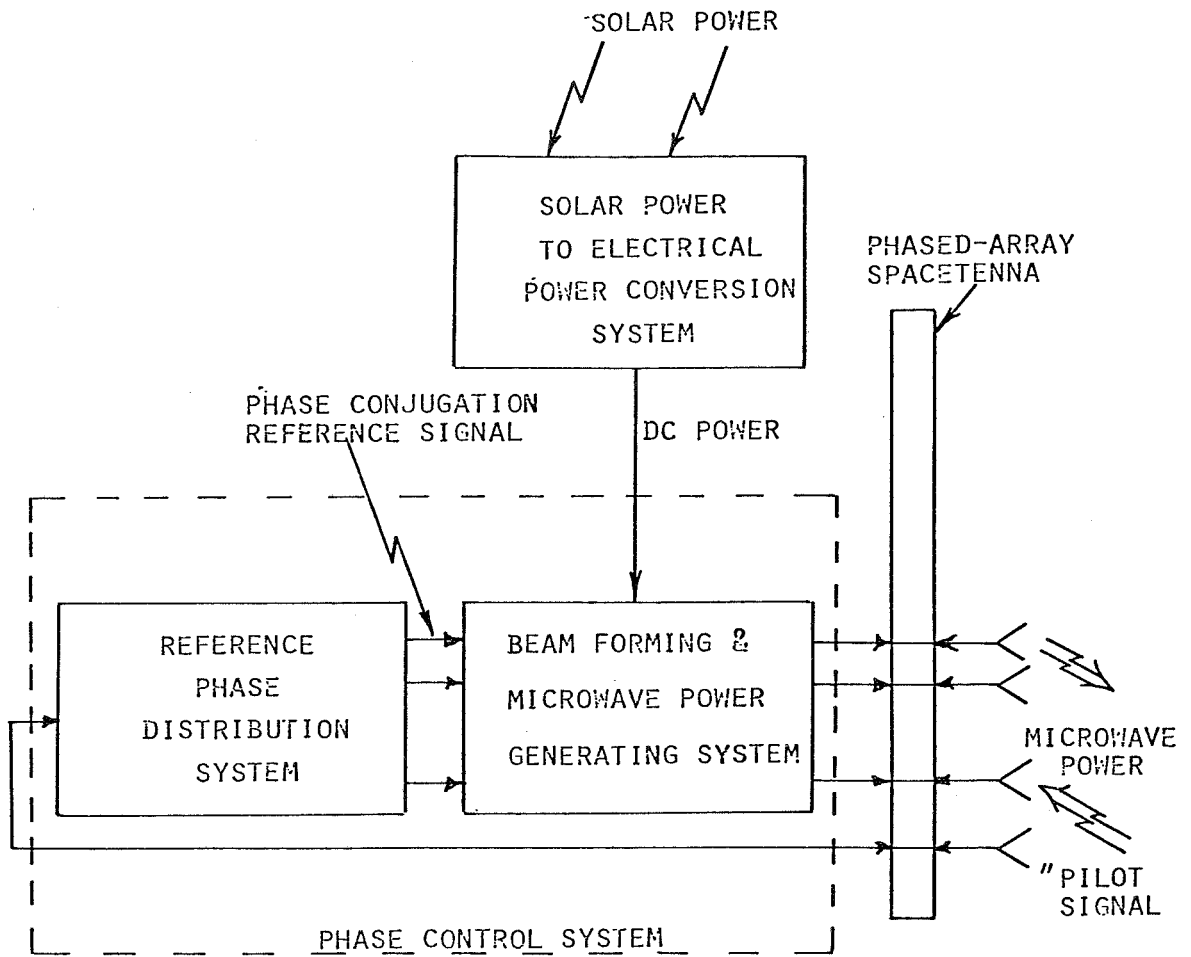
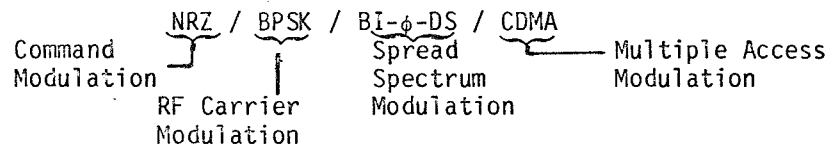


Figure 2.2. Solar Power Satellite (SPS) Transmission System (Phase Conjugation).

from Fig. 2.2 the SPS Transmission System consists of three major systems: (1) The Reference Phase Distribution System, (2) The Beamforming and Microwave Power Generating System, and (3) The Solar Power to Electrical Power Conversion System.

2.2 Reference System SPS-Pilot Waveform

The reference system SPS pilot waveform utilizes: (1) NRZ command modulation, (2) split phase, direct sequence pseudo-noise or spread spectrum modulation, BI- ϕ -DS. This combined data-code modulation is used to bi-phase modulate (BPSK) the RF carrier. Multiple access in the SPS network is to be achieved via code division multiple access techniques (CDMA). Thus the baseline SPS pilot waveform is characterized via four modulation components summarized by the symbols:



A functional diagram indicating the mechanization of the pilot transmitter is shown in Fig. 2.3. As illustrated the data clock and code clock are coherent so that the uplink operates in a data privacy format. The purpose of the spread spectrum (SS) code generator is several fold. First it provides link security, second it provides a multiple access capability for the operation of a network of SPSs, and third, the anti-jamming protection is provided for both intentional radio frequency interference (RFI) and unintentional RFI such as those arising from a neighboring SPS on the adjacent orbit. Proper choice of this code modulation will also provide the needed isolation between the uplink and the downlink, since a notch filter can be placed around the carrier frequency at the SPS receiver input to blank out the interferences without destroying the uplink signal (see pilot signal spectrum in Fig. 2.3). The selection of the PN code parameters to achieve the code isolation and processing gain required will be addressed in Section 3.

2.3 Reference-Phase Control-System

The reference phase control system concept was presented in detail in Ref. 3; its major features are summarized in this section. Based upon earlier study efforts (Refs. 3,4), a phase control system concept has been proposed which partitions the system into three major levels. Figure 2.4 demonstrates the partitioning and represents an expanded version of Fig. 2.2. The first level in Fig. 2.4 consists of a reference phase distribution system implemented in the form of phase distribution tree structure. The major purpose of the tree structure is to electronically compensate for the phase shift due to the transition path lengths from the center of the spacetenna to each phase control center (PCC) located in each subarray. In the reference system, this is accomplished using the Master Slave Returnable Timing System (MSRTS) technique. The detailed mathematical modeling and analysis of the MSRTS technique is provided in Ref. 4. Based upon extensive tradeoffs

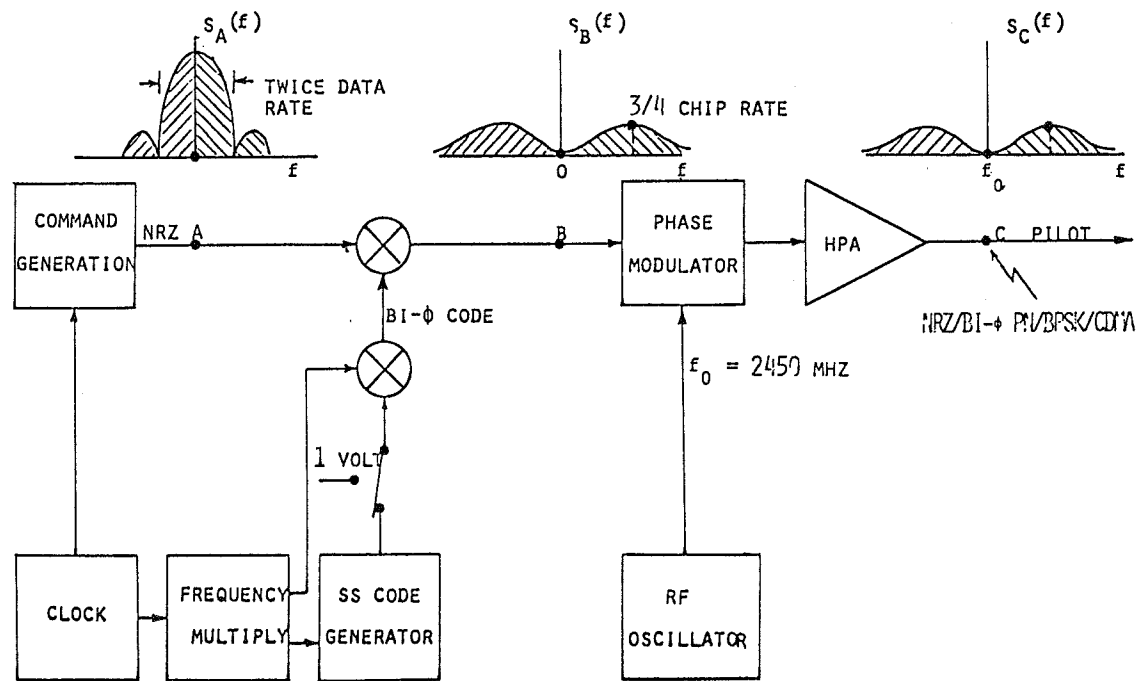


Figure 2.3. Reference System Pilot Signal Transmitter Functional Diagram.

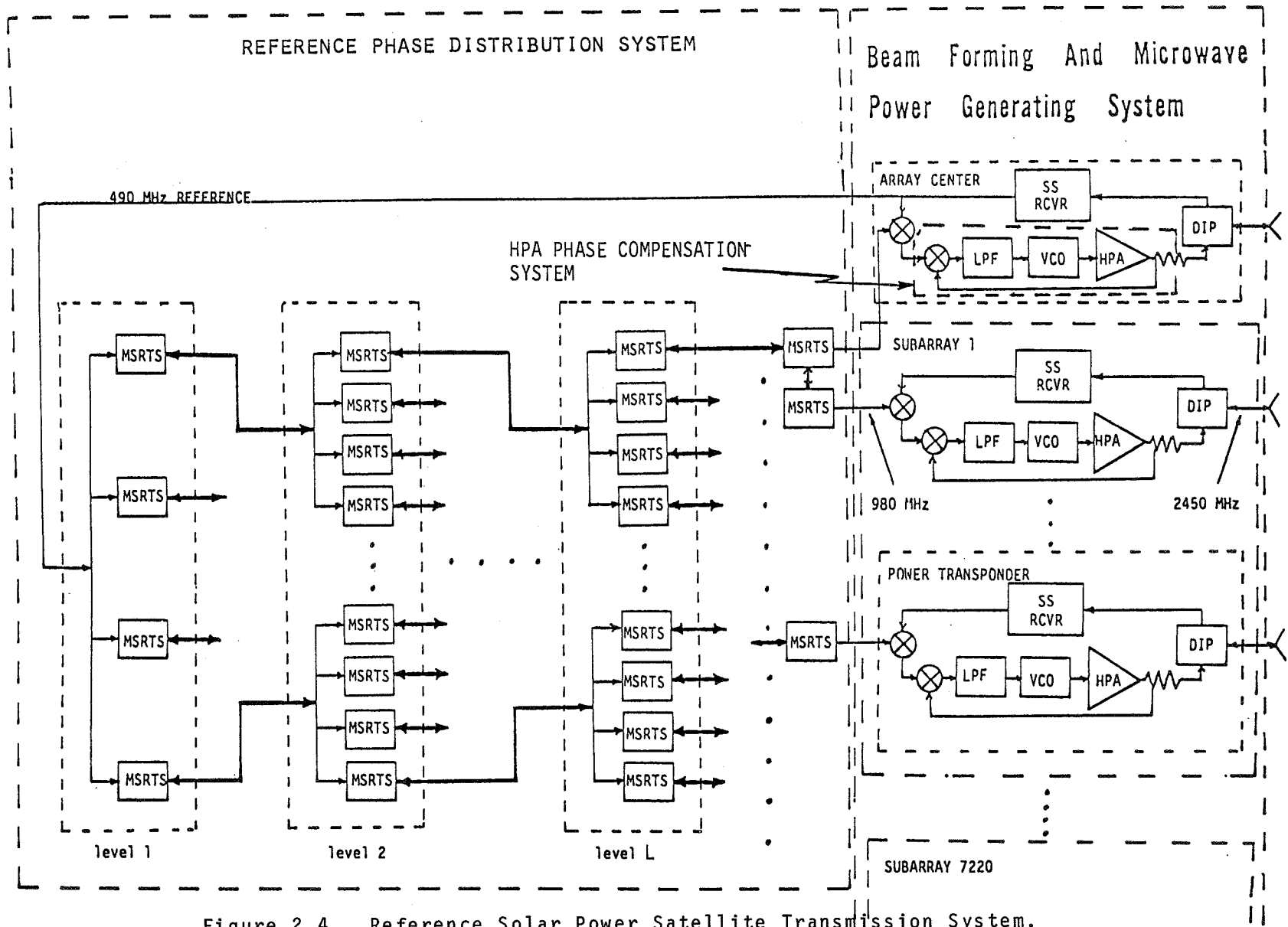


Figure 2.4. Reference Solar Power Satellite Transmission System.

using SOLARSIM and appropriate analysis during the Phase II study, a four level tree is selected to be the reference phase distribution system configuration.

The second level is the Beam Steering and Microwave Power Generation System which houses the SPS Power Transponders. This transponder consists of a set of phase conjugation multipliers driven by the reference phase distribution system output and the output of a pilot spread spectrum receiver (SS RCVR) which accepts the received pilot via a diplexer connected to a separate receive horn or the subarray itself. The output of the phase conjugation circuits serve as inputs to the third level of the phase control system. The third level of phase control is associated with maintaining an equal and constant phase shift through the microwave power amplifier devices while minimizing the associated phase noise effects (SPS RFI potential) on the generated power beam. This is accomplished by providing a phase-locked loop around each high power amplifier.

2.4 Reference System-SPS-Power Transponder

In addition to distributing the constant phase reference signal over the spacetenna, a method for recovering the phase of the received pilot signal is required. Figure 2.5 represents the functional diagram of the SPS power transponder. This includes the pilot signal receiver, phase conjugation electronics and the high power amplifier phase control system.

In the mechanization of the SPS power transponders, two receiver "types" will be required; however, most of the hardware will be common between two receivers. One receiver, the Pilot Spread Spectrum Receiver, is located at the center of the spacetenna or the reference subarray. It serves two major functions: (1) acquires the SS code, the carrier and demodulates the command signal, (2) provides the main input signal to the Reference Phase Distribution System.

The second receiver "type" will be located in the Beam Forming and Microwave Power Generating System. Its main purpose is to phase conjugate the received pilot signal and transpond power via the j-th spacetenna element, $j = 1, 2, \dots, 101, 552$.

In the case that data transmitting capability is not implemented for the pilot signal, the Costas loop can be replaced by a CW loop. This avoids the need for provisions to resolve the associated Costas loop induced phase ambiguity.

3.0 PILOT SIGNAL DESIGN AND POWER TRANSPONDER ANALYSIS

The key technical problem areas concerning the reference phase control system design and specifications are the SPS pilot signal design and power transponder analysis. Figure 3.1 illustrates the radio frequency interference (RFI) scenario.

The interferences are generated by different mechanisms: (1) self jamming due to the power beam leakage from the diplexer/circulator; (2) mutual coupling from adjacent transponders, (3) thermal noise and (4)

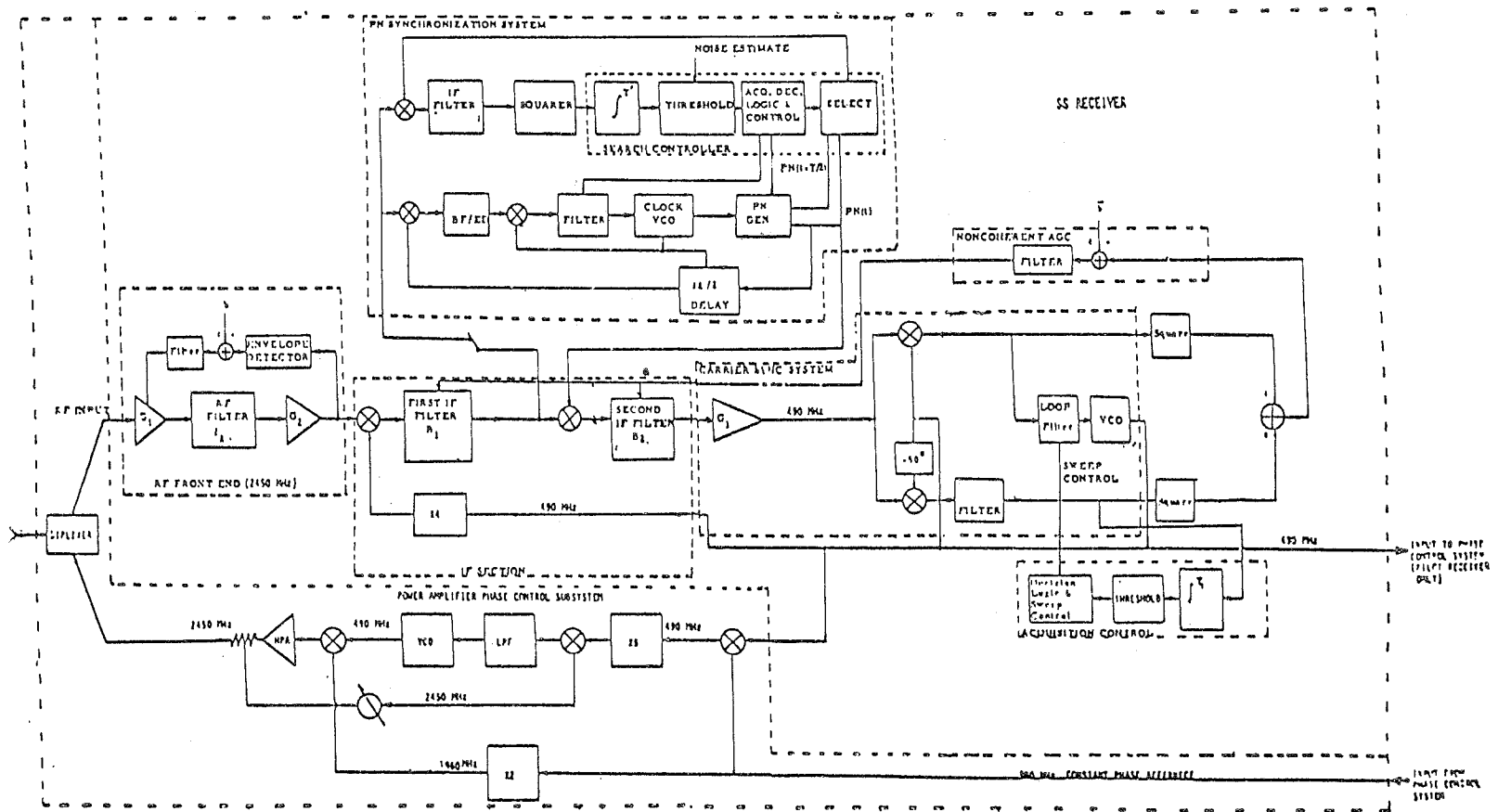
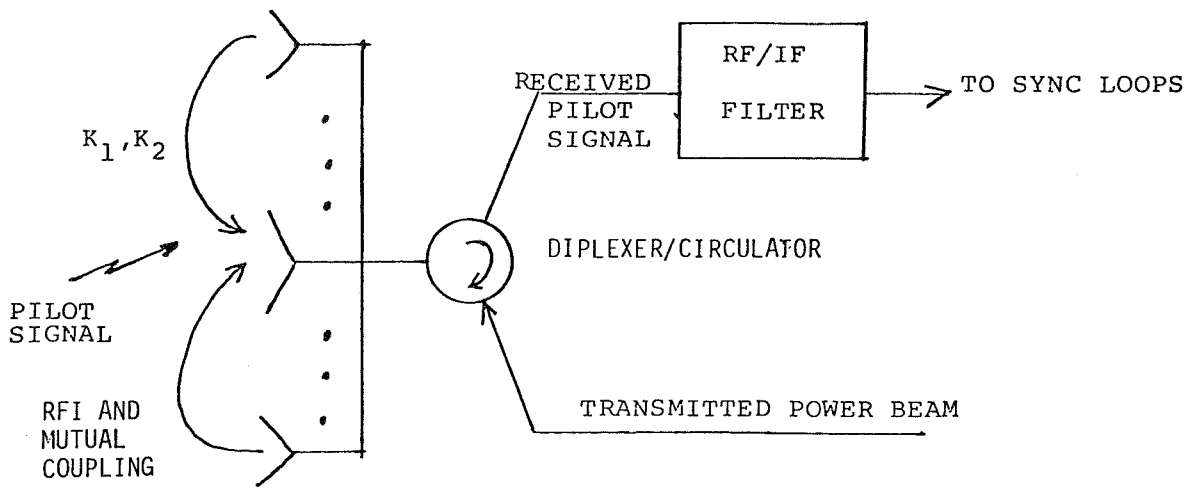
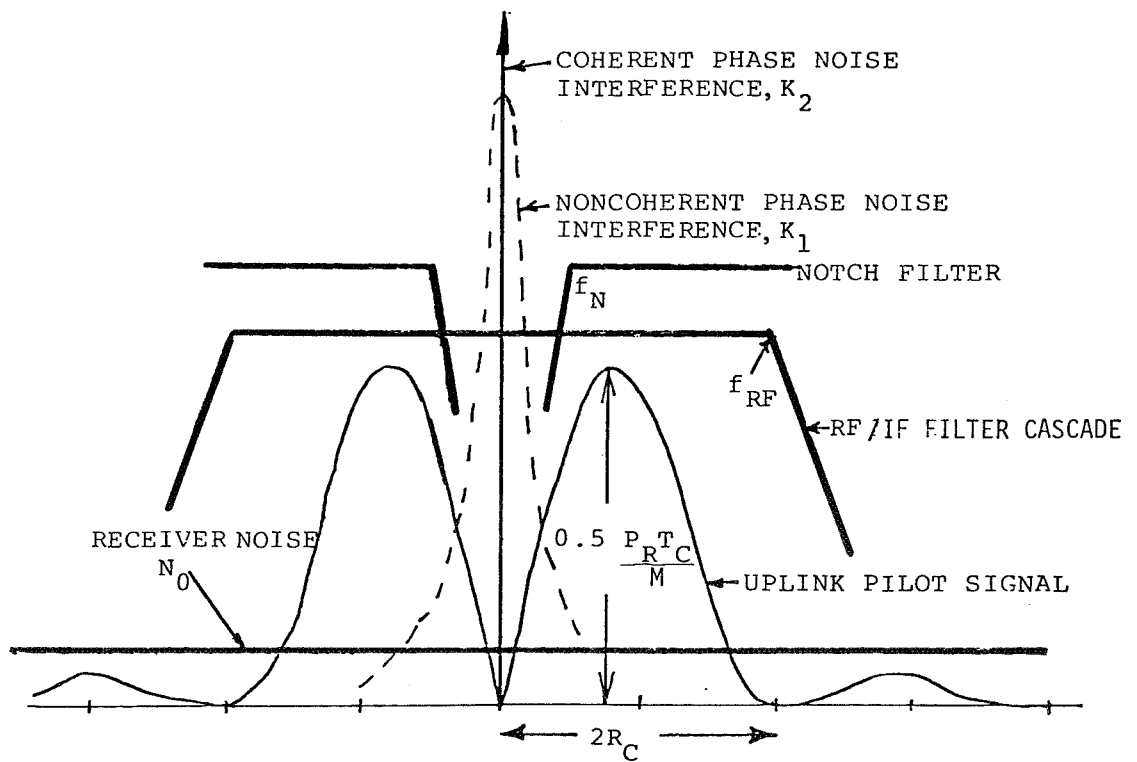


Figure 2.5. Central SPS Power Transponder Located at Spacetenna Center.



(a) SPS Power Transponder Front End (Conceptual)



(b) Signal and Noise Spectrum

Figure 3.1. Signal and Noise Spectrum into SPS Transponder.

interference from adjacent SPSs. The signal and interference spectrum at the input to the SPS transponder is depicted in Fig. 3.1. In general, the combined phase noise interference from the power beams consists of a coherent and a noncoherent term. Depending on the mechanization of the antenna structure and diplexer/circulator characteristics, these terms are associated with gains K_1 and K_2 . Note that the phase noise interferences are concentrated around the carrier frequency (2450 MHz). The uplink pilot signal on the other hand has no power around this frequency. Its power spectrum peaks at $f = 0.75 R_c$, with a value proportional to the produce of the received power (P_r) and the PN chip rate (R_c), and inversely proportional to the PN code length (M). The parameters R_c and M are related to the processing gain of the PN spread signal and determines its interference suppression capability. The RF filter characteristic is mainly determined by the waveguide antennas, which have bandwidths ranging from 15 to 45 MHz depending on the array area. Our goal is to optimally select (1) the pilot signal so that it passes the RF filter with negligible distortions, and (2) a practical notch filter that rejects most of the phase noise interferences. When this is done, one can be assured that the reconstructed pilot signal phase after the sync loops is within a tolerable error for the retrodirective scheme.

3.1 Pilot Signal Parameter Selection

SOLARSIM is developed to enable performance tradeoffs of pertinent design parameters such as pilot signal transmitter EIRP, PN code requirement, chip rate and RF front end characteristics (notch filter). The computer model is based upon a mathematical framework which includes the analytical models for power spectral density of the pilot signal, various sources of interference, the RF front end, the PN tracking loop and the pilot tracking loop. The resulting design values are provided in a later section.

3.2 Power Transponder Analysis

Analytical models are developed for the SPS transponder tracking loop system that include: (1) the PN desreader loop, (2) the pilot phase tracking (Costas) loop and (3) the PA phase control loop. The phase reference receiver that feeds the phase distribution system is also modeled. Various sources of potential phase noise interferences are identified and their effects on the performance of the individual loops are modeled. In particular, a model of the phase noise profile of the klystron amplifier based on a specific tube measurement is introduced. Important implications on the PA control loop design are also addressed.

An analytical model for evaluating the overall performance of the SPS transponder is given. The phase fluctuation at the output of the transponder is shown to be directed related to the various noise processes through the closed-loop transfer functions of the tracking loops. These noise processes are either generated externally to the transponder circuitry such as ionospheric disturbances, transmit frequency instability, or externally such as receiver thermal noise, power beam interferences, data distortions, VCO/mixer phase noise and the phase variations introduced by the reference distribution tree.

3.3 Summary of Results

The important findings and preliminary specifications the transponder design parameters and results based upon SOLARSIM and the analytical models discussed in Sections 3.1 and 3.2 can be summarized as follows:

- EIRP = 93.3 dBW
- PN Chip Rate ~ 10 Mcps
- RF filter 3 dB cutoff frequency ~ 20 MHz
- Notch filter 3 dB cutoff frequency ~ 1 MHz
- Notch filter dc attenuation ~ 60 dB
- PN Code period ~ 1 msec
- Costas loop phase jitter < 0.1 deg for 10 Hz loop bandwidth
- Channel Doppler is negligible
- Klystron phase control loop bandwidth > 10 kHz

In arriving at these design values, we have used extensively the capabilities of SOLARSIM to perform the necessary tradeoffs. Figure 3.2 represents a typical design curve generated via SOLARSIM and used to pick the RF filter 3 dB cutoff frequency. The details and other tradeoffs performed are documented in Ref. 5, Vol. II.

The preliminary results are generated using a tentative model of RFI with coupling coefficients $K_1 = K_2 = 20$ dB. Explicitly, we assumed that the transponder input sees a CW interference with power equal to 0.65 KW and a phase noise (1/f type) interference at about 20 W. Of course, when these values are changed significantly, our predictions have to be modified. For this reason, the development and verification of an acceptable model for the effects of mutual coupling on the phase array antenna based upon the "near field" theory is extremely important and essential in the near future.

A maximum-length linear-feedback shift register sequence, i.e., m-sequences generated by a 12 stage shift register with a period equal to 4095 is recommended as the spread spectrum code. In the code division multiple access situation, the theoretical optimal solution is to use the set of 64 bent function sequences of period 4095, enabling as much as 4095 simultaneous satellite operation of the SPS network. The bent sequences are guaranteed to be balanced, have long linear span and are easy to initialize. However, the set of maximum length sequence of period 4095, though suboptimal, may suffice. This depends of course on the code partial correlation requirement and the number of satellites in the network. The design detail is discussed in Ref. 5, Vol. II.

At this point our results indicate that it is feasible to hold the antenna array phase error to less than one degree per module for the type of disturbances modeled in this report. However, there are irreducible error sources that are not considered herein and their effects remain to be seen. They include: (a) reference phase distribution errors. (b) differential delays in the RF path.

4.0 SPS PERFORMANCE EVALUATION VIA SOLARSIM

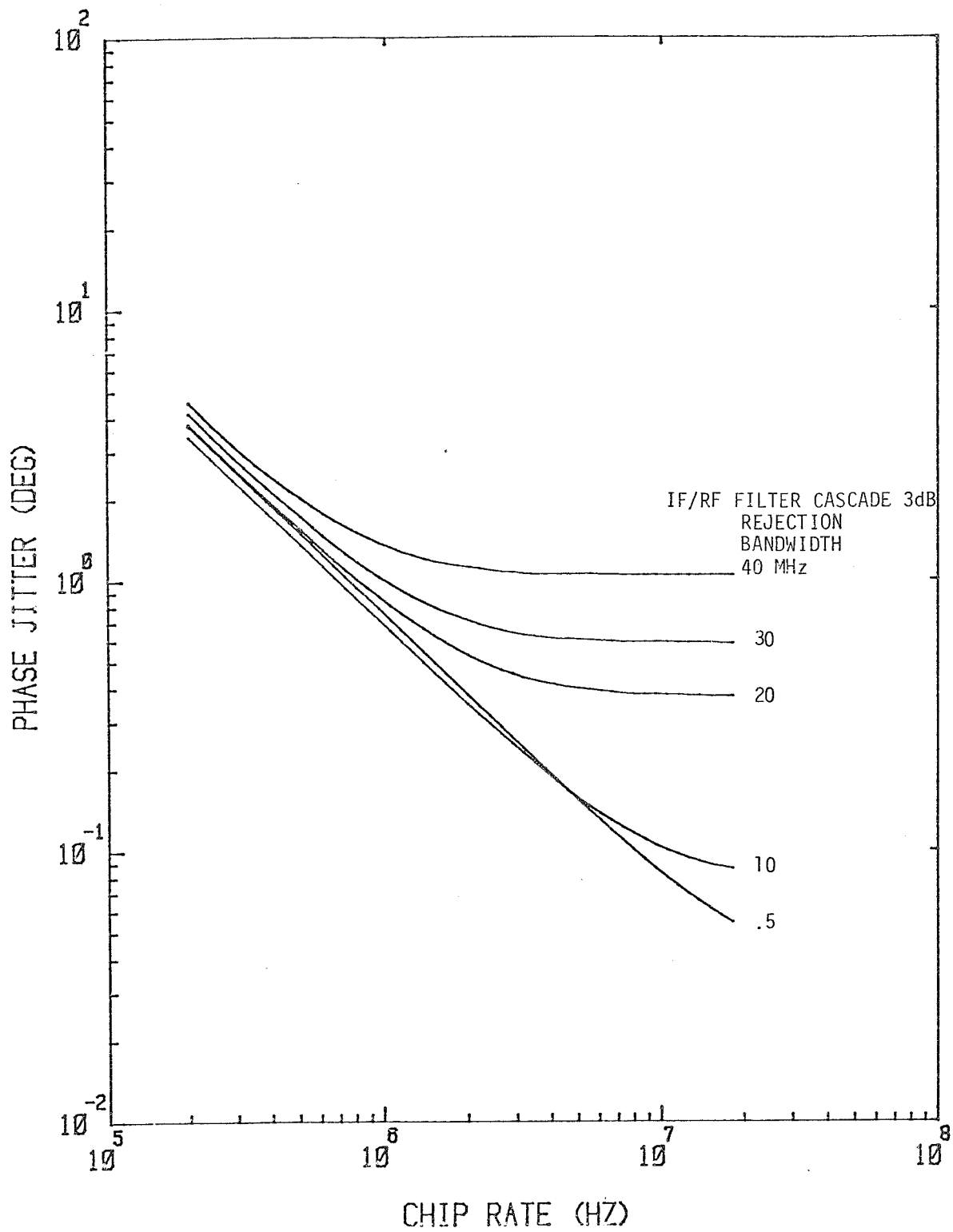


Figure 3.2. Effect of Varying Notch Filter Frequency Cutoff.

Because of the complicated nature of the problem of evaluating performance of the SPS phase control system and because of the multiplicity and interaction of the problems as they relate to subsystem interfaces, the methods of analysis and computer simulation (analytical simulation) have been combined to yield performance of the SPS system. The result is the development of SOLARSIM--a computer program package that allows a parametric evaluation of critical performance issues. The SOLARSIM program and its various subroutines have been exercised in great detail to provide system engineering tradeoffs and design data for the reference system. In what follows, we shall focus on the key results obtained from one of the SOLARSIM subroutines, viz., POWER TRANSFER EFFICIENCY.

4.1 System Jitters and Imperfections Modeled in POWER TRANSFER EFFICIENCY

The system jitters and imperfections can be grouped into two main classes: (1) jitters arising due to spacetenna electrical components which include such effects as the amplitude jitter and the phase jitters of the feed currents and (2) jitters arising due to the mechanical imperfections of the spacetenna which include the subarray tilts (mechanical pointing error), tilt jitters and the location jitters. The location jitters include the transmitting and receiving elements and arise from the misplacement of the radiating elements.

4.2 Definition of Power Transfer Efficiency

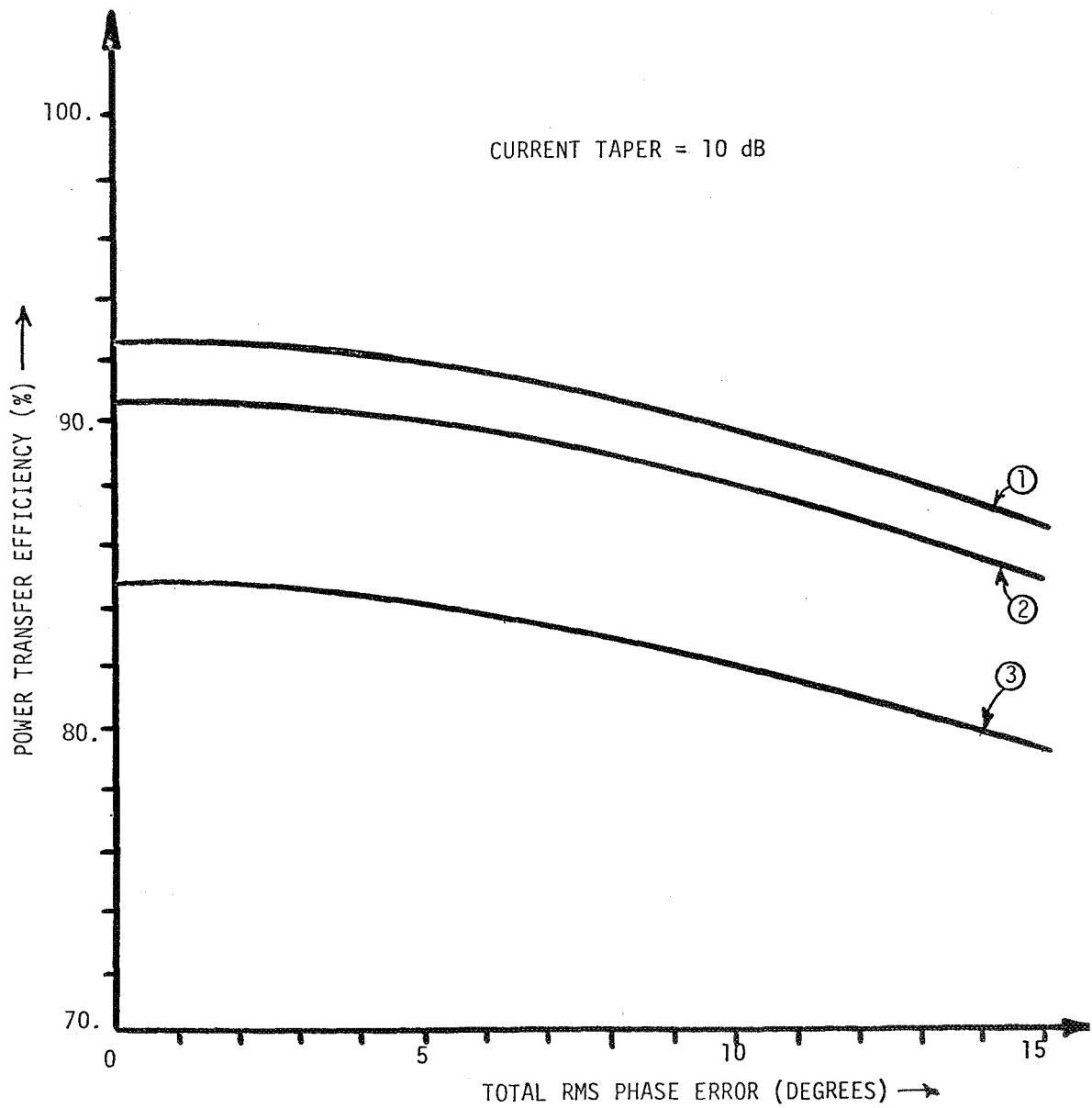
The power transfer efficiency adopted is defined by:

$$\text{POWER TRANSFER EFFICIENCY} = \frac{\text{Power Received by the 10 km Diameter Rectenna}}{\text{Total Power Radiated by the Spacetenna}}$$

This definition is convenient because the multiplying constants due to the propagation through the medium cancel out from the numerator and denominator.

4.3 Effects of System Imperfections on SPS Efficiency

Figures 4.2 - 4.3 summarize the effects of the various system imperfections on the SPS power transfer efficiency obtained through SOLARSIM. In Figure 4.1, the power transfer efficiency is plotted against the total phase error produced by the SPS phase control system. For a mechanically perfect system with no location jitters and mechanical pointing errors or jitters (curve ①), the total rms phase error is restricted to less than 10^0 at RF to yield a 90% efficiency. Curve ② depicts the influence of the mechanical pointing error (assumed to be $10'$ with a jitter of $2'$) when the location jitters are absent. As can be seen from the figure, for a total phase error of 10^0 the power transfer efficiency of the spacetenna drops down to 87.3%. When the location jitters of 2% of lambda is added for the transmitting and receiving elements, this number drops down to 82.0% (see Curve ③). It is expected that the SPS system will operate in the region between Curve ① and ③. In this case, the power transfer efficiency will be less than 90% for a typical rms phase error of 10 degrees.



LEGEND

- ① MECHANICAL POINTING ERROR (MPE) = 0, LOCATION JITTER (LJ) = 0, JITTER ON MECHANICAL POINTING = 0
- ② MPE = 10', LJ = 0, JITTER ON MPE = 2'
- ③ MPE = 10', LJ = 2% of λ , JITTER ON MPE = 2'

Figure 4.1. SPS Power Transfer Efficiency vs Phase Error.

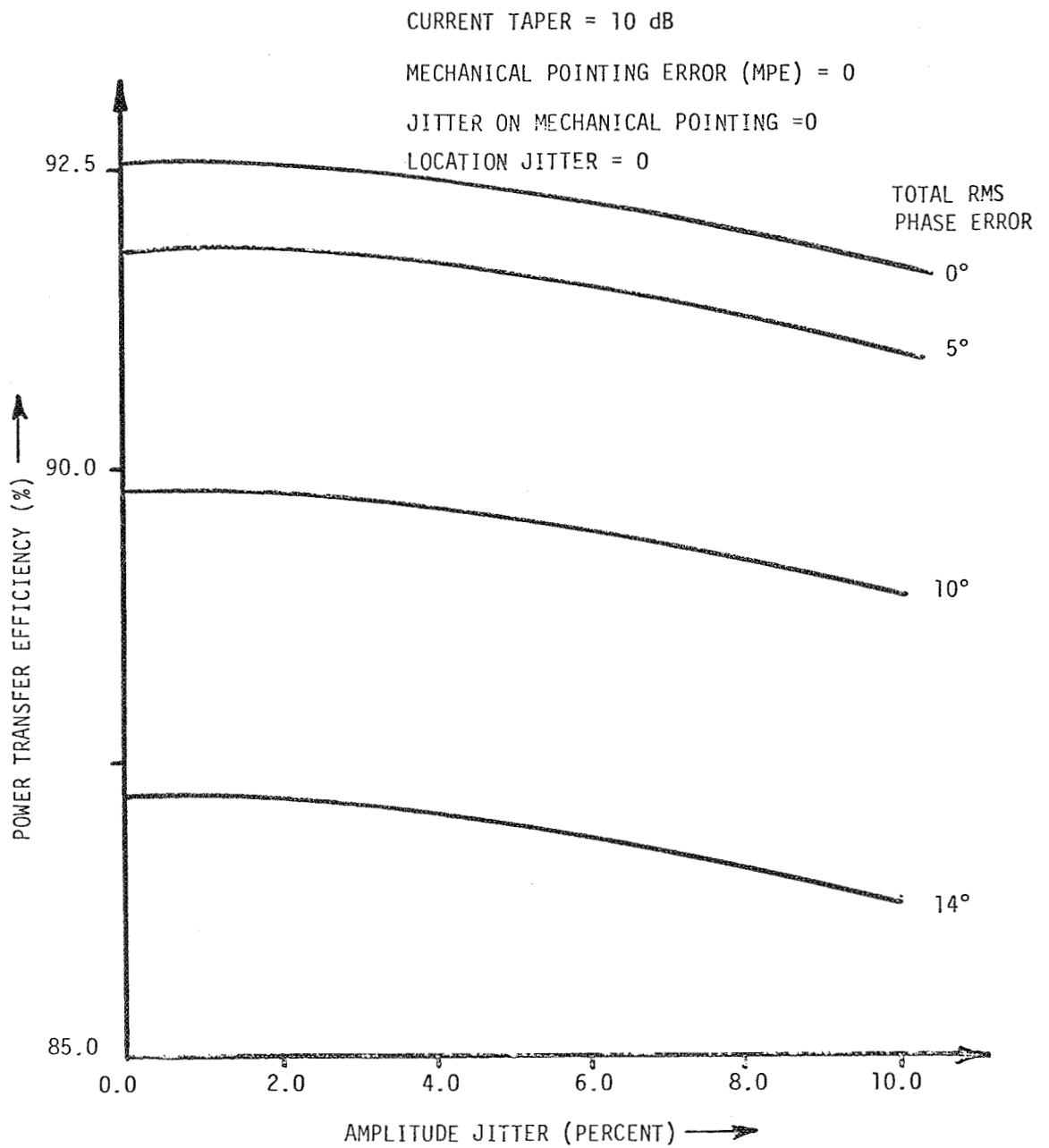


Figure 4.2. Effect of Amplitude Jitter on SPS Power Transfer Efficiency.

CURRENT TAPER = 10 dB
MECHANICAL POINTING ERROR = 0
JITTER ON MECHANICAL POINTING = 0
PHASE JITTER = 0

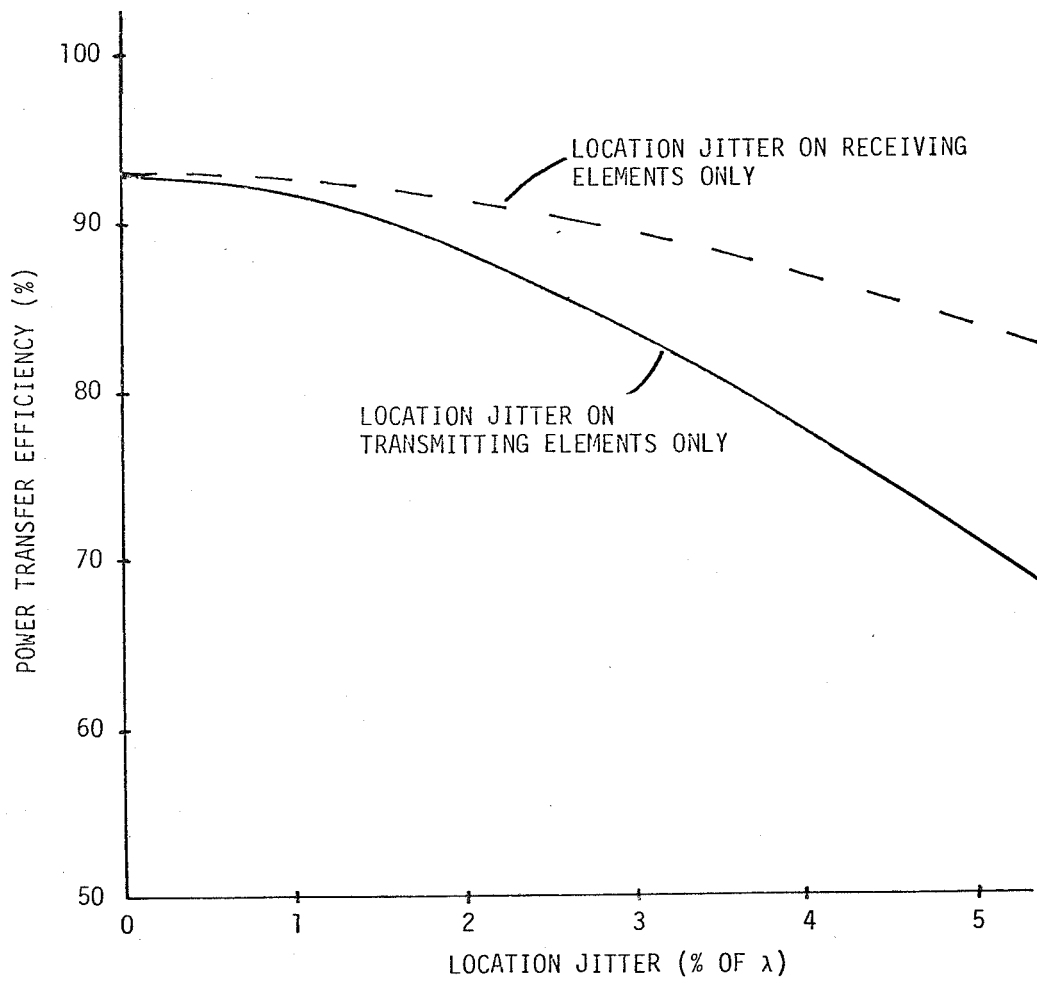


Figure 4.3 Effect of Location Jitters on the Otherwise Perfect SPS.

4.3.1 Current Amplitude Jitter

The effect of the current amplitude jitter is shown in Fig. 4.2 for a mechanically perfect system. As can be seen from the figure, for an amplitude jitter of 5%, the power transfer efficiency of the mechanically perfect spacetenna with the current phase jitter of 0° is 92.3%. This value drops to 91.63% for the total phase error of 5° and to 89.57% for a total phase error of 10° . One can conclude that the power transfer efficiency is relatively insensitive to the amplitude jitters.

4.3.2 Location Jitters

Figure 4.3 investigates the effects of location jitters on the power transfer efficiency of an otherwise perfect SPS. As can be seen from the figure, the degradation of efficiency is severe: for a location jitter on each radiating element of $2\% \lambda$ the power transfer efficiency drops to 88.3%. As a comparison, Fig. 4.1 shows that for a rms phase error of 7° ($2\% \lambda = 7.2^\circ$) the efficiency is down to 91.2%. It is noticeable that the effect produced by location jitters on the receiving (conjugating) elements is comparable to the effect produced by the phase error. This is true because both these effects enter into the transmission system at the same physical point, i.e., the center subarray. On the other hand, power transfer efficiency is rather sensitive to the location jitter on the radiating elements.

REFERENCES

1. Lindsey, W. C., and Kantak, A. V., "Automatic Phase Control in Solar Power Satellite Systems," Prepared for NASA/JSC, TR-7809-0977, September 1977, LinCom Corporation, P.O. BOX 2793D, Pasadena, CA.
2. Lindsey, W. C., "A Solar Power Satellite Transmission System Incorporating Automatic Beam Forming, Steering and Phase Control," prepared for NASA/JSC, TR-7806-0977, June 1978, LinCom Corporation, P.O. BOX 2793D, Pasadena, CA.
3. Lindsey, W. C., and Kantak, A. V., "Automatic Phase Control in Solar Power Satellite Systems," Prepared for NASA/JSC, TR-7802-0977, February 1978, LinCom Corporation, P.O. BOX 2793D, Pasadena, CA.
4. Lindsey, W. C., Kantak, A. V., Chie, C. M., and Booth, R. W. D., "SPS Phase Control System Performance Via Analytical Simulation, Phase II," Prepared for NASA/JSC, TR-7903-0977, March 1979, LinCom Corporation, P.O. BOX 2793D, Pasadena, CA.
5. Lindsey, W. C., Kantak, A. V., and Chie, C. M., "SPS Phase Control Performance Via Analytical Simulation Phase III," Vols. I-IV, Prepared for NASA/JSC, TR-0180-0779, January 1980, LinCom Corporation, P. O. BOX 2793D, Pasadena, CA.